PHYSICAL REVIEW D **84,** 036009 (2011)

Tau lepton charge asymmetry and new physics at the LHC

Sudhir Kumar Gupta* and German Valencia†

Department of Physics, Iowa State University, Ames, Iowa 50011, USA

(Received 11 February 2011; revised manuscript received 11 July 2011; published 15 August 2011)

We consider the possibility of studying new physics that singles out the tau lepton at the LHC. We concentrate on the tau lepton charge asymmetry in $\tau^+\tau^-$ pair production as a tool to probe this physics beyond the standard model. We consider two generic scenarios for the new physics. We first study a nonuniversal Z' boson as an example of a new resonance that can single out tau leptons. We then consider vector lepto-quarks coupling the first-generation quarks with the third-generation leptons as an example of nonresonant new physics. We find that in both cases the charge asymmetry can be sufficiently sensitive to the new physics to provide useful constraints at the LHC.

DOI: 10.1103/PhysRevD.84.036009 PACS numbers: 11.30.Er, 11.30.Hv, 12.60.Cn, 13.35.Dx

I. INTRODUCTION

The Large Hadron Collider (LHC) has been running since earlier last year in an initial phase of rediscovering the standard model (SM). A variety of observables are necessary to completely measure the SM couplings and we concentrate here on the charge asymmetry, the hadron collider equivalent of the familiar forward-backward asymmetry. During the early stages of LHC running, the available event rates will possibly allow measurements of lepton charge asymmetries near the Z peak. These translate into measurements of the weak angle, $\sin^2\theta_W$, and can help in the SM rediscovery phase at LHC.

When the LHC is running at its design energy and luminosity, it will be possible to extend these measurements to higher regions of dilepton-invariant mass, $M_{\ell\ell}$, not probed by LEP-II, and in this way play an important role in the search for new physics. The Drell-Yan dilepton pair production process is important in this context due to its clean signature. In this paper we discuss the use of the lepton charge asymmetry as a tool to discover and identify new physics, with emphasis on the τ-pair production channel.

There exists a vast literature dedicated to the study of new physics associated with the top quark, that is motivated by its large mass and possible unique role in electroweak symmetry breaking. It is natural to ask whether new physics that singles out the top quark does not in fact single out the whole third generation of the SM fermions. This is particularly the case in light of the existing anomaly in the forward-backward asymmetry of the b quark .

With this in mind, we wish to explore the possibility of new physics that affects the tau lepton but does not show up in studies of muons or electrons. To this effect we consider two different scenarios that single out the third-generation leptons. The scenarios are not complete models, but instead they describe two simple possibilities. Our first example is a nonuniversal Z' which has been studied before in connection with the top quark [2]. Here we explore its consequences in tau lepton physics at the LHC in the large tau-pair-invariant mass, $M_{\tau\tau}$ region. It is possible that such a Z' can be detected by simply looking for bumps in the $M_{\tau\tau}$ distribution, but we emphasize here the question of detecting its effect via the lepton charge asymmetry. Our second example consists of vector lepto-quarks which provide a benchmark for effects from nonresonant new physics. By associating the third family of leptons with the first family of quarks, the lepto-quarks in question single out the tau lepton [3].

We first present a study at the τ-lepton level in Sec. III. In Sec. IV, we back up our conclusions by considering selected τ-lepton decay modes.

II. CHARGE ASYMMETRY (FORWARD-BACKWARD ASYMMETRY)

Forward-backward asymmetries have proven to be valuable tools for constraining the SM and searching for new physics in e^+e^- colliders. A prominent example is the A_{FB}^b anomaly measured at LEP [4], which remains a hint for new physics [1]. More recently the Tevatron has reported an anomaly in the forward-backward asymmetry of the top quark [5] which has also received considerable attention [6].

Forward-backward asymmetries can still be defined for the LHC even though it is a symmetric pp collider. The idea is to consider processes that are initiated by $q\bar{q}$ annihilation at the parton level. It is then possible to define the forward-backward asymmetry in the usual way in the parton center-of-mass frame (CM): the forward direction corresponding to the incoming quark direction. To connect with the pp collider, it is sufficient to recall that the quarks in the proton carry, on average, a larger fraction of the proton momentum than the antiquarks; the direction of the quark momentum is thus correlated with the direction of the total momentum of the event in the lab frame (the boost direction).

*skgupta@iastate.edu
†valencia@iastate.edu

Specifically, one can start from the parton CM asymmetry defined in the usual way

$$\mathcal{A}_{FB}^{\star}(q\bar{q} \to \ell^- \ell^+) \equiv \frac{\sigma_F - \sigma_B}{\sigma_F + \sigma_B}, \tag{1}$$

where σ_F (σ_B) is the respective cross section for producing a lepton ℓ^- that travels forward (backward) with respect to the initial quark direction. This has been studied by both the ATLAS [7] and CMS [8] collaborations in connection with measurements of $\sin^2\theta_W$ from the SM asymmetries at the Z peak.

In the lab frame, a nonvanishing $\mathcal{A}_{FB}^{\star}$ will manifest itself as a rapidity asymmetry: the forward leptons in the parton center-of-mass will have a larger rapidity in the lab frame. At the LHC, the symmetry of the initial pp state results in a quark direction that is equally likely to correspond to either proton. The net effect of an $\mathcal{A}_{FB}^{\star}$ in the lab frame at the LHC is a charge asymmetry in which the type of lepton that preferred the backward direction in the CM now concentrates in the central rapidity region. This charge asymmetry is in a sense equivalent to a forward-backward asymmetry, but defined in lab frame for a symmetric pp collider.[1]

Following this argument, it is common to define a charge asymmetry in terms of the fermion rapidity [9,10]. In our case,

$$\mathcal{A}(y) = \frac{N_{\ell^+}(y) - N_{\ell^-}(y)}{N_{\ell^+}(y) + N_{\ell^-}(y)}, \tag{2}$$

where y is rapidity of the lepton $\ell^\pm$ and N is the number of events with a given rapidity y. One advantage of using this charge asymmetry over the forward-backward asymmetry in Eq. (1) is that the parton CM frame does not need to be reconstructed, as this reconstruction is not always possible. It is also common to define an integrated asymmetry over a central region, limited by y_c:

$$\mathcal{A}_c(y_c) = \frac{N_{\ell^+}(-y_c \le y \le y_c) - N_{\ell^-}(-y_c \le y \le y_c)}{N_{\ell^+}(-y_c \le y \le y_c) + N_{\ell^-}(-y_c \le y \le y_c)}. \tag{3}$$

This integrated asymmetry can be optimized with a carefully chosen y_c [9]. Notice that the symmetry of the initial pp state at LHC causes the integrated asymmetry to vanish when the whole rapidity range is used. Finally, it may be convenient to integrate the charge asymmetry over different ranges of $M_{\ell\ell}$ as we discuss below.

III. MODEL DESCRIPTIONS AND NUMERICAL ANALYSIS

In this section we describe briefly the two models we use to illustrate the effectiveness of the charge asymmetry and we present the corresponding numerical results. These two models are chosen because we are mostly interested in applications to τ-lepton physics at LHC and both are examples of new physics that singles out the τ-lepton.

In all cases we use HADGRAPH 4.4.39 [11] for event generation and PYTHIA 6.4.21 [12] for the analysis. To this end we implement the vertices that originate in each of the two new physics models directly into HADGRAPH. We use CTEQ6L-1 parton distribution functions [13]. We also implement the basic acceptance cuts $p_{T_\tau} > 20$ GeV, $|\eta_\tau| < 2.5$, and $\Delta R_{\tau\tau} > 0.4$. Our results will show that the measurements we propose will not be possible in the early running of LHC. For this reason we will assume a τ physics program when LHC is running at $\sqrt{S} = 14$ TeV center-of-mass energy, and with an integrated luminosity of 10 fb^{-1} per year.

We first carry out our analysis at the τ-lepton level, without concerning ourselves with the subsequent τ decays. This will serve to assess the best case scenario of high efficiency τ-lepton tagging and reconstruction as both CMS and ATLAS expect to be able to detect τ-leptons with relatively large efficiencies [14,15]. We will then partially address these issues by considering a few selected τ-lepton decay modes.

The SM itself produces a nonzero charge asymmetry so that a search for new physics involves measuring the deviation from the SM. Depending on the new physics, this deviation may be small and a precise measurement may be needed.

We begin with a discussion of the charge asymmetry in the SM. Within the SM, dileptons at the LHC are produced

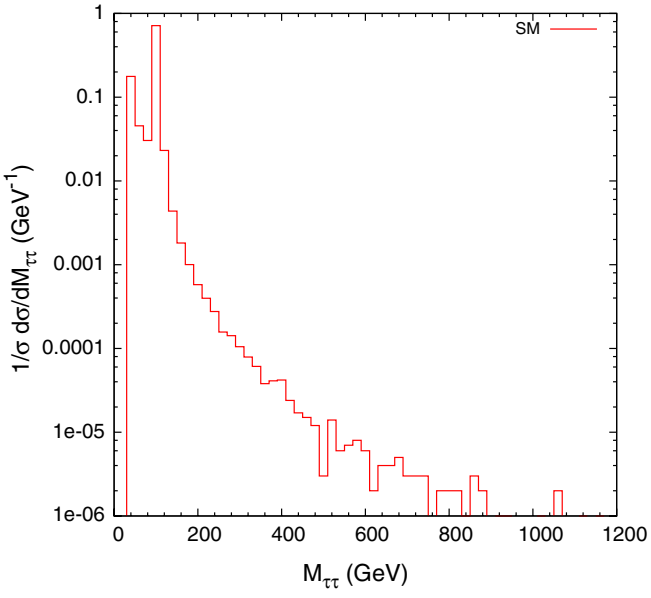

FIG. 1 (color online). Dilepton-invariant mass distribution for the process $pp \to \tau^+\tau^-$ within standard model at the LHC for $\sqrt{S} = 14$ TeV.

[1]This charge asymmetry should not be confused with the unequal production rates for W^+ and W^- in pp colliders.

predominantly via s-channel exchange of a photon or a Z boson with a total cross section (for our acceptance cuts) of $\sim$941 pb at $\sqrt{S} = 14$ TeV. The corresponding SM $\tau^+\tau^-$ events exhibit an $M_{\tau\tau}$ distribution shown in Fig. 1. This differential cross section exhibits a clear Z peak and falls rapidly with $M_{\tau\tau}$. To distinguish possible new physics it is therefore useful to exclude the Z region and to look as far out in $M_{\tau\tau}$ as the event rate permits. We will find that the best region to look for new physics (at least in the two examples we consider) is $M_{\tau\tau} > 200$ GeV.

Our main observable is the integrated charge asymmetry over both rapidity, within a range determined by $|y| < y_c$, and $M_{\tau\tau} > M_{\rm min}$. Previous studies related to the top quark have shown that there is an optimal value for y_c in Eq. (3) [9] and we illustrate this point within the context of the SM in Fig. 2. This figure indicates that values around $y_c \sim 0.5$ maximize the integrated charge asymmetry more or less independently from the $M_{\rm min}$ value used. The selection of $M_{\rm min}$ proceeds as discussed above: we want to exclude the Z peak region to minimize the effect of the SM as a background to the new physics without reducing the event rate too much. It turns out that the asymmetry increases with increasing $M_{\rm min}$ (at least up to the $M_{\rm min} = 300$ GeV that we have tested) and this is illustrated in Fig. 2. As $M_{\rm min}$ increases, this cut is more effective in rejecting events with a lower boost and this results in an increased asymmetry. The choice of a specific value for $M_{\rm min}$ will thus result from a compromise between a somewhat larger asymmetry and reduced statistics as $M_{\rm min}$ increases. We explore this further when we discuss results within the illustrative models.

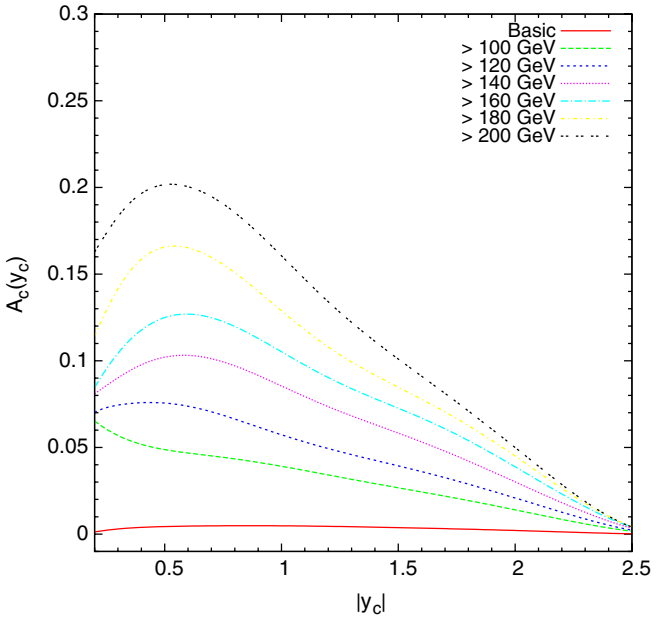

FIG. 2 (color online). Integrated charge asymmetry for the standard model with basic acceptance cuts as well as different minimum dilepton-invariant mass cuts.

A. Nonuniversal Z' model

One of the most frequently studied extensions of the SM is an additional $U(1)'$ symmetry and its associated Z' boson [16]. Although the $U(1)'$ charges are family universal in most of the models discussed in the literature, this need not be the case. It is well known that a nonuniversal Z' induces tree-level flavor-changing neutral currents (FCNC) which are severely constrained by experiment, most notably meson mixing [17].

In this paper we will not concern ourselves with the FCNC, but rather with the possibility of an enhanced coupling to the τ-lepton as in the models of Refs. [18,19], that can be probed at LHC.

We write the general couplings of a nonuniversal Z' boson to the SM fermions as follows,

$$\mathcal{L}_{Z'} = \frac{g}{2\cos\theta_W}(\bar{f}\gamma^\mu(c_L^f P_L + c_R^f P_R)f)Z'_\mu. \qquad (4)$$

In Eq. (4), g and θ_W denote, as usual, the weak $SU(2)_L$ coupling constant and the electroweak mixing angle respectively; $P_{L,R}$ are $(1 \pm \gamma_5)/2$; and the strength of the new interaction is parameterized by $c_{L,R}^f$. A model with an enhanced coupling $c_{L,R}^\tau$ singles out the τ-lepton pair production process. Of course, at LHC, we also need to know how the Z' is produced and this forces us to specify its couplings to light quarks.

We consider enhanced Z' couplings to the third generation that are accompanied by correspondingly suppressed couplings to the light generations as happens in the models mentioned above. This results in a complete $q\bar{q} \to \tau^+\tau^-$ process that is of electroweak strength. Existing constraints on this Z' are twofold. From the LEP-II process $e^+e^- \to \tau^+\tau^-$ considering both the cross section and the forward-backward asymmetry as a function of $M_{\tau\tau}$, Ref. [19] concludes that masses $M_{Z'} \lesssim 500$ GeV are excluded. The phenomenology of such a Z' at LHC *vis-à-vis* its enhanced couplings to the top quark has also been considered both for flavor-conserving [2], as well as flavor-violating processes [20]. It was found that the simple Drell-Yan-type processes are completely overwhelmed by QCD background. Processes with three or four top (or bottom) quarks at the LHC could constrain the model for Z' masses up to

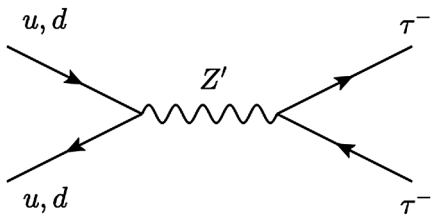

FIG. 3. Representative Feynman diagram for dilepton production through Z' exchange.

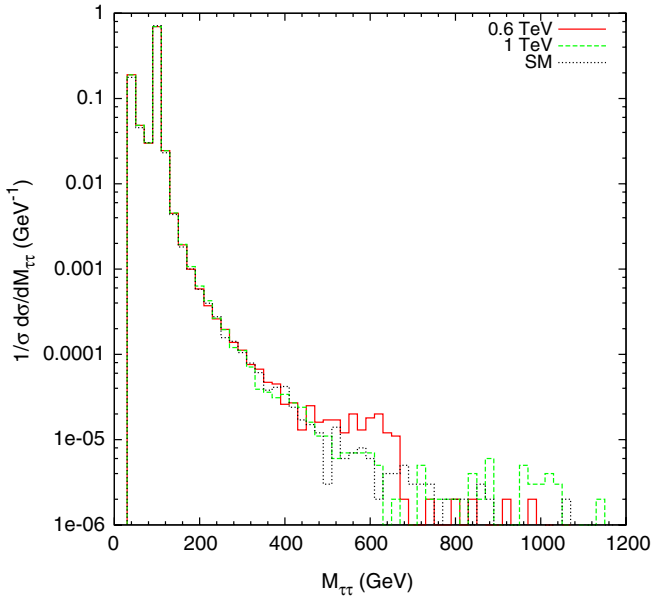

FIG. 4 (color online). Dilepton-invariant mass distributions for the Z'-model at the LHC with $\sqrt{S} = 14$ TeV for $M_{Z'} = 0.6$ and 1 TeV.

2 TeV, but several hundred fb^{-1} of integrated luminosity would be necessary.

In this model, the additional contribution to the partonic process $q\bar{q} \to \ell^+\ell^-$ is due to an s-channel Z' exchange as shown in the Fig. 3. We consider two cases, corresponding to $M_{Z'} = 600$ GeV and $M_{Z'} = 1$ TeV. In both cases we will use a relatively narrow Z' width of 100 GeV. For illustration purposes we use purely right-handed couplings with overall strength $c_R^u \cdot c_R^\tau = 1/3$.

TABLE I. Dilepton pair cross sections (in pb) for the Z' model and the SM at the LHC with $\sqrt{S} = 14$ TeV. All the masses shown here are given in TeV.

Cuts	Z' Model		SM
	$M_{Z'} = 0.6$	$M_{Z'} = 1$	
Basic	948.9 ± 1.3	948.6 ± 1.3	941.0 ± 1.2
$M_{\tau\tau} > 0.2$ TeV	1.58 ± 0.002	1.49 ± 0.002	1.41 ± 0.002

In Fig. 4 we present the resulting $M_{\tau\tau}$ distribution for the two values of the Z' mass, 600 GeV and 1 TeV, as well as for the SM. As Table I shows, removing the low $M_{\tau\tau}$ region results in a significant loss of events. However, Fig. 4 illustrates that in the region of low ditau-invariant mass the SM completely obscures the new physics. To increase the sensitivity to new physics we therefore need to remove this low invariant ditau mass region, especially the Z peak.

If there is a new resonance, such as a Z', with a mass in the energy range accessible to LHC it could be discovered by studying the cross section or an invariant mass distribution such as that shown in Fig. 4. We do not address this possibility in this paper as this is not the focus of our study. Our focus is the charge asymmetry: if sufficiently different from the SM prediction it could signal new physics that is not directly observable as a resonance (for example, because it is too heavy). The charge asymmetry is a very useful observable even if new physics is first discovered as a resonance: it would serve to distinguish between different possibilities as we illustrate below. We therefore begin by asking whether the Z' can yield a charge asymmetry that

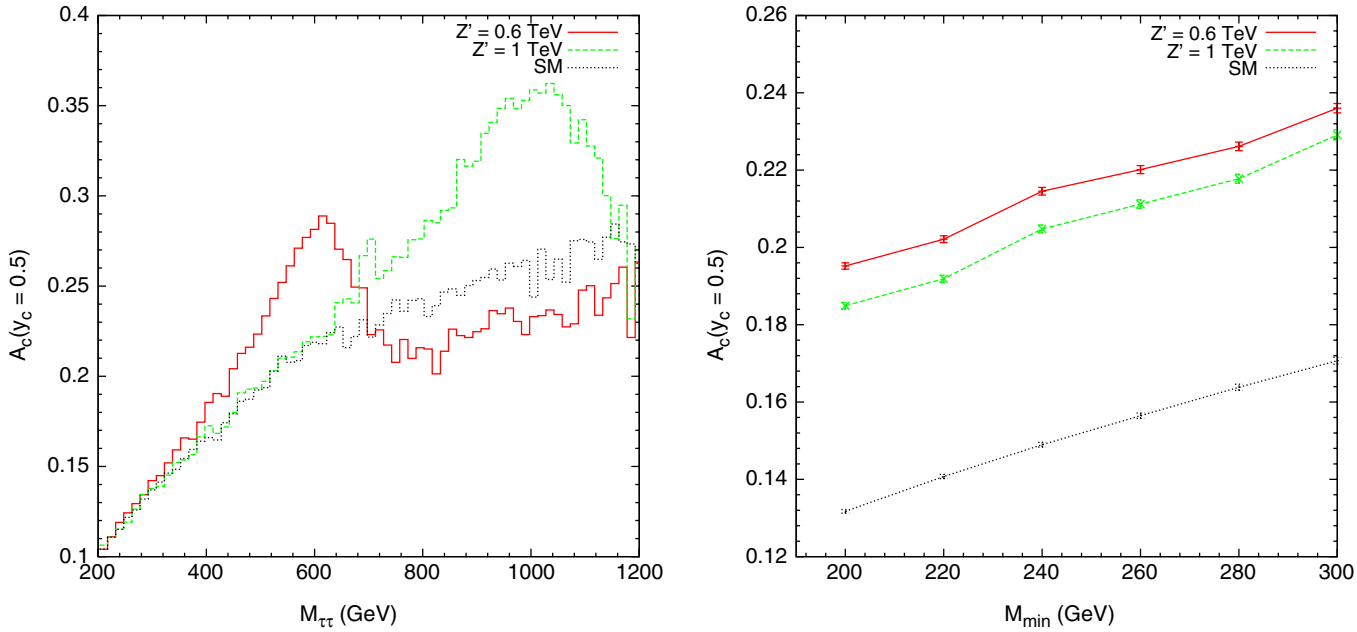

FIG. 5 (color online). Lepton charge asymmetry in the Z' model for $M_{\tau\tau} > 200$ GeV, $y_c = 0.5$ and $M_{Z'} = 0.6$ and 1 TeV vs $M_{\tau\tau}$ (left) and integrated over $M_{\tau\tau} \geq M_{\min}$ (right). This model has only nonzero couplings as c_R^τ, and c_R^u such that $c_R^\tau \cdot c_R^u = 1/3$.

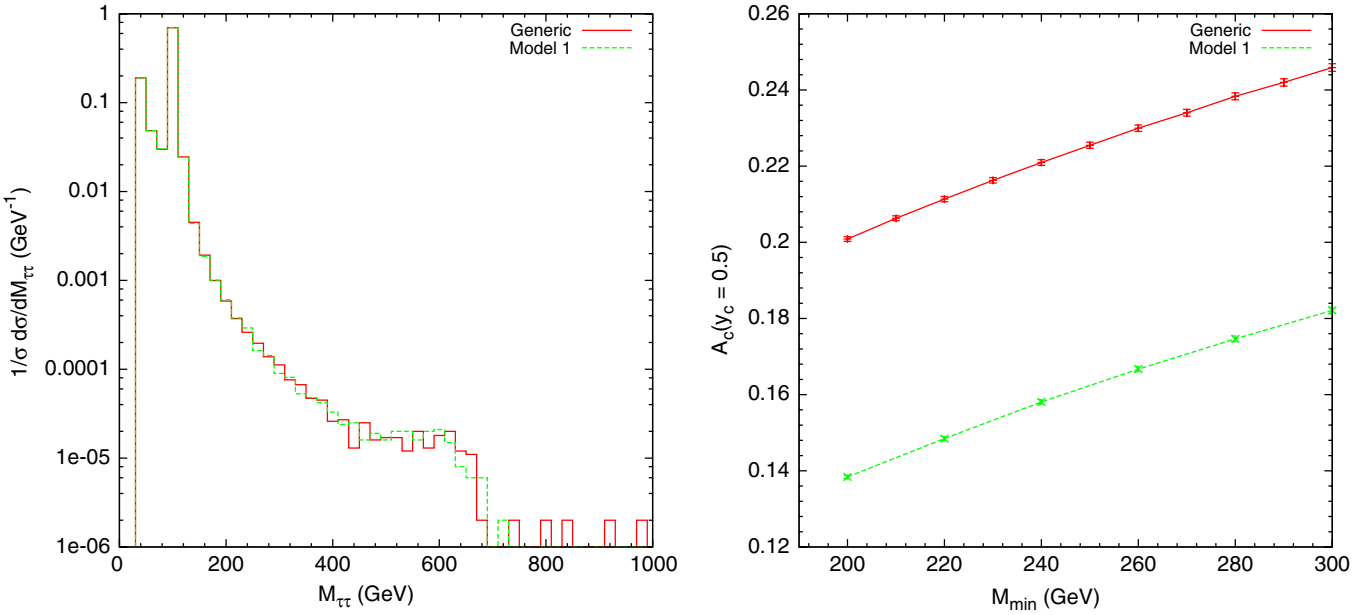

FIG. 6 (color online). Comparison of two Z' models with $M_{Z'} = 600$ GeV in invariant mass distribution $M_{\tau\tau}$ (left) and integrated charge asymmetry (right). The model labeled "Generic" has only nonzero couplings c_R^τ and c_R^u such that $c_R^\tau \cdot c_R^u = 1/3$. The model labeled "Model 1" is that of Ref. [2].

differs sufficiently from the SM to be observed. This is illustrated in Fig. 5.

The first figure shows the charge asymmetry for $y < y_c = 0.5$ as a function of dilepton-invariant mass. The second figure shows the corresponding asymmetry integrated over dilepton-invariant mass, as a function of $M_{\rm min} \gtrsim 200$ GeV.

We have explored the effect of variations in the couplings to some extent. Coupling the Z' to d-quarks instead of u-quarks for its production process diminishes its contributions at LHC. Replacing the purely right-handed coupling with a purely left-handed coupling affects the interference between the SM and the Z'. In Fig. 6 we emphasize the utility of the charge asymmetry in helping to untangle any possible new physics that may first be observed in the invariant mass distribution. We compare two Z' cases both with mass 600 GeV: the generic case described above, where the only nonzero couplings are c_R^τ, and c_R^u such that $c_R^\tau \cdot c_R^u = 1/3$; and the model studied in Ref. [2]. As is evident from the figure, the two models have nearly identical invariant mass distributions but significantly different integrated charge asymmetry.

To quantify these results further we study the statistical sensitivity of the LHC to these signals. In Table II we show the integrated τ-lepton charge asymmetry in percent for the two values of the Z' mass as well as for the SM. We show results for several values of $M_{\rm min}$ for $y_c = 0.5$ with their corresponding 1σ statistical error. These errors correspond to accumulated statistics for 10 fb^{-1} at $\sqrt{S} = 14$ TeV. We can see that the asymmetry increases (both for the SM and the Z' model) as we increase $M_{\rm min}$, but the error also increases due to the correspondingly reduced statistics.

TABLE II. Integrated lepton charge asymmetry (in percent), $\mathcal{A}_c(y_c)$, for the Z' model and the SM. The 1σ errors correspond to statistics for one year of LHC data (at $\int \mathcal{L} dt = 10$ fb^{-1} per year). All the masses here are given in TeV. In this Table the Z' model's only nonzero couplings are c_R^τ, and c_R^u such that $c_R^\tau \cdot c_R^u = 1/3$.

Cuts	Z' Model		SM
	$M_{Z'} = 0.6$	$M_{Z'} = 1$	
$M_{\tau\tau} > 0.20$ TeV	20.1 ± 0.6	19.6 ± 0.6	13.2 ± 0.6
$M_{\tau\tau} > 0.22$ TeV	21.1 ± 0.7	20.6 ± 0.7	14.1 ± 0.7
$M_{\tau\tau} > 0.24$ TeV	22.1 ± 0.8	21.5 ± 0.8	14.9 ± 0.8
$M_{\tau\tau} > 0.26$ TeV	23.0 ± 0.8	22.5 ± 0.9	15.6 ± 0.9
$M_{\tau\tau} > 0.28$ TeV	23.8 ± 1.0	23.3 ± 1.0	16.4 ± 1.0
$M_{\tau\tau} > 0.30$ TeV	24.6 ± 1.0	24.1 ± 1.1	17.1 ± 1.1

B. Lepto-quark models

As a second example of new physics that singles out τ-lepton pairs at LHC we consider lepto-quarks. This example will serve to illustrate the case where the new physics does not have a resonant peak in the channel of interest.

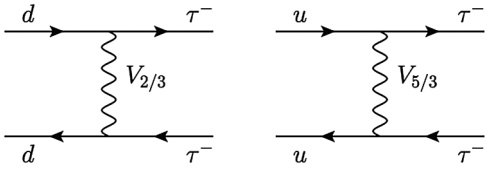

FIG. 7. Feynman diagram for dilepton production through lepto-quark exchange in lepto-quark Model 1 (left) and 2 (right).

TABLE III. Dilepton pair cross sections (in pb) for lepto-quark model 1, 2 (LQ-1, 2) and, the SM at the LHC with $\sqrt{S} = 14$ TeV. All the masses shown here are given in TeV.

Cuts	LQ-1		LQ-2		SM
	$M_{V_{2/3}} = 0.6$	$M_{V_{2/3}} = 1$	$M_{V_{5/3}} = 0.6$	$M_{V_{5/3}} = 1$	
Basic	938.1 ± 1.3	938.4 ± 1.3	918.5 ± 1.4	912.9 ± 1.3	941.0 ± 1.2
$M_{\tau\tau} > 0.2$ TeV	2.06 ± 0.002	1.43 ± 0.002	4.70 ± 0.002	2.21 ± 0.002	1.41 ± 0.002

Generic couplings of vector lepto-quarks to standard model fermions can be written in the form [21]

$$\begin{aligned}\mathcal{L}_{\mathrm{LQ}} = \mathcal{L}_{\mathrm{SM}} &+ \lambda^{(R)}_{V_0} \cdot \bar{d}\gamma^\mu P_R e \cdot V^{R\dagger}_{0\mu} \\ &+ \lambda^{(R)}_{\tilde{V}_0} \cdot \bar{u}\gamma^\mu P_R e \cdot \tilde{V}^{\dagger}_{0\mu} + \lambda^{(R)}_{V_{1/2}} \cdot \bar{d}^c\gamma^\mu P_L \ell \cdot V^{R\dagger}_{1/2\mu} \\ &+ \lambda^{(R)}_{\tilde{V}_{1/2}} \cdot \bar{u}^c\gamma^\mu P_L \ell \cdot \tilde{V}^{\dagger}_{1/2\mu} + \lambda^{(L)}_{V_0} \cdot \bar{q}\gamma^\mu P_L \ell \cdot V^{L\dagger}_{0\mu} \\ &+ \lambda^{(L)}_{V_{1/2}} \cdot \bar{q}^c\gamma^\mu P_R e \cdot V^{L\dagger}_{1/2\mu} + \lambda^{(L)}_{V_1} \cdot \bar{q}\gamma^\mu P_L V^{\dagger}_{1\mu} \ell \\ &+ \mathrm{H.c.} \end{aligned} \tag{5}$$

In the equation above V^j_i are vector lepto-quarks with weak isospins $i = 0, 1/2, 1$ coupled to left-handed ($j = L$) or right-handed ($j = R$) quarks, respectively. The cases with weak isospin $i = 0, 1/2$ admit two possible values of hypercharge (leading to different electric charges), we denote the two possibilities by V and $\tilde{V}$. Scalar lepto-quarks are also possible [22].

For our study, we have in mind Pati-Salam [23] type lepto-quarks in which the coupling $\lambda^{(R)}_{V_0} = \lambda^{(L)}_{V_0} = g_s/\sqrt{2}$ at the unification scale, where g_s is the strong coupling constant. In order to single out the τ-lepton we envision a scenario described in Ref. [3] in which the third generation of leptons is associated with the first generation of quarks.

For our numerical analysis we will only consider the following two types of lepto-quark as an illustration:

(i) LQ-1, a Pati-Salam lepto-quark as described above with coupling $\lambda^{(R)}_{V_0} = \lambda^{(L)}_{V_0} = g_s/\sqrt{2}$ between the first-generation quarks and the third-generation leptons. This leads to $\tau^+\tau^-$ pairs produced by $\bar{d}d$ annihilation at LHC. The lepto-quark V_0 in this case has electric charge $2/3$ so we refer to it as $V_{2/3}$.

(ii) LQ-2, with coupling $\lambda^{(R)}_{\tilde{V}_0} = g_s/\sqrt{2}$ between the first-generation quarks and the third-generation leptons. This one is a variation of LQ-1 in which the $pp \to \tau^+\tau^-$ process is initiated by $u\bar{u}$ annihilation (instead of $d\bar{d}$ in LQ-1). The lepto-quark $\tilde{V}_0$ in this case has electric charge $5/3$ so we refer to it as $V_{5/3}$.

Although lepto-quarks with these particular flavor quantum numbers are not commonly discussed, generic direct bounds on vector lepto-quark masses are in the hundreds of GeV range [24]. It is well-known, however, that rare decays place stronger indirect constraints, for example [25]. For the specific flavor couplings we use here, Ref. [3] identified the process $B_s \to \mu e$ as the one yielding the tightest constraint.

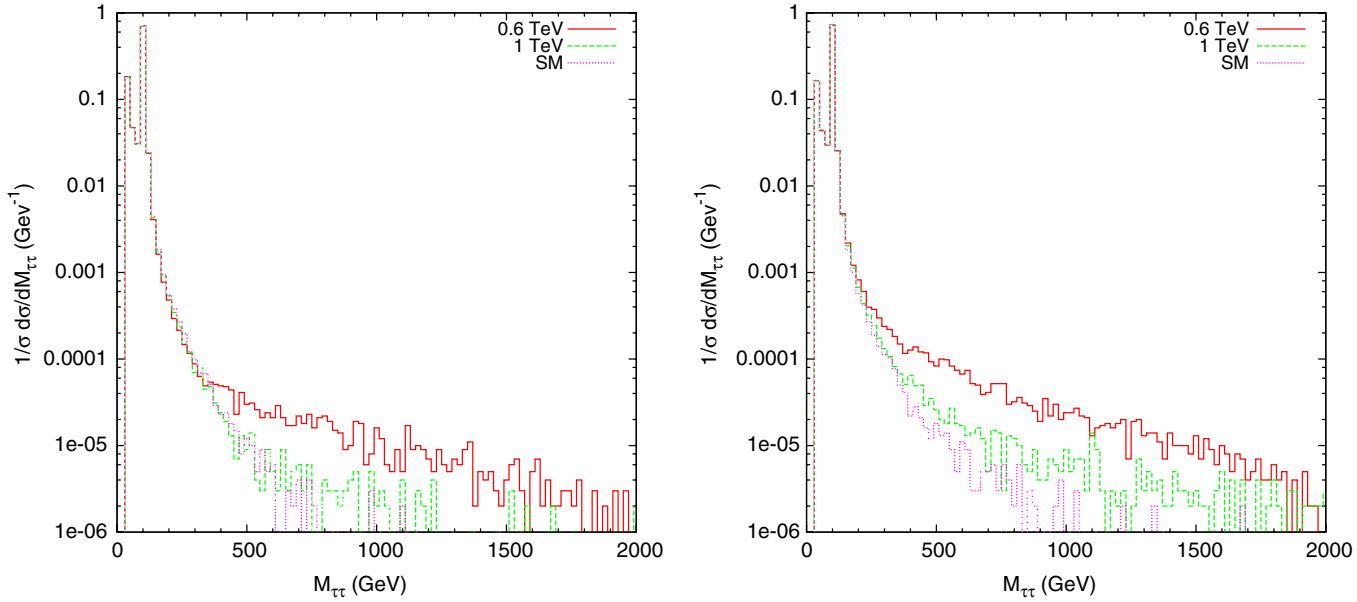

FIG. 8 (color online). Dilepton-invariant mass distributions for the scenarios LQ-1 and LQ-2 at the LHC with $\sqrt{S} = 14$ TeV for $M_{\mathrm{LQ}} = 0.6$ and 1 TeV.

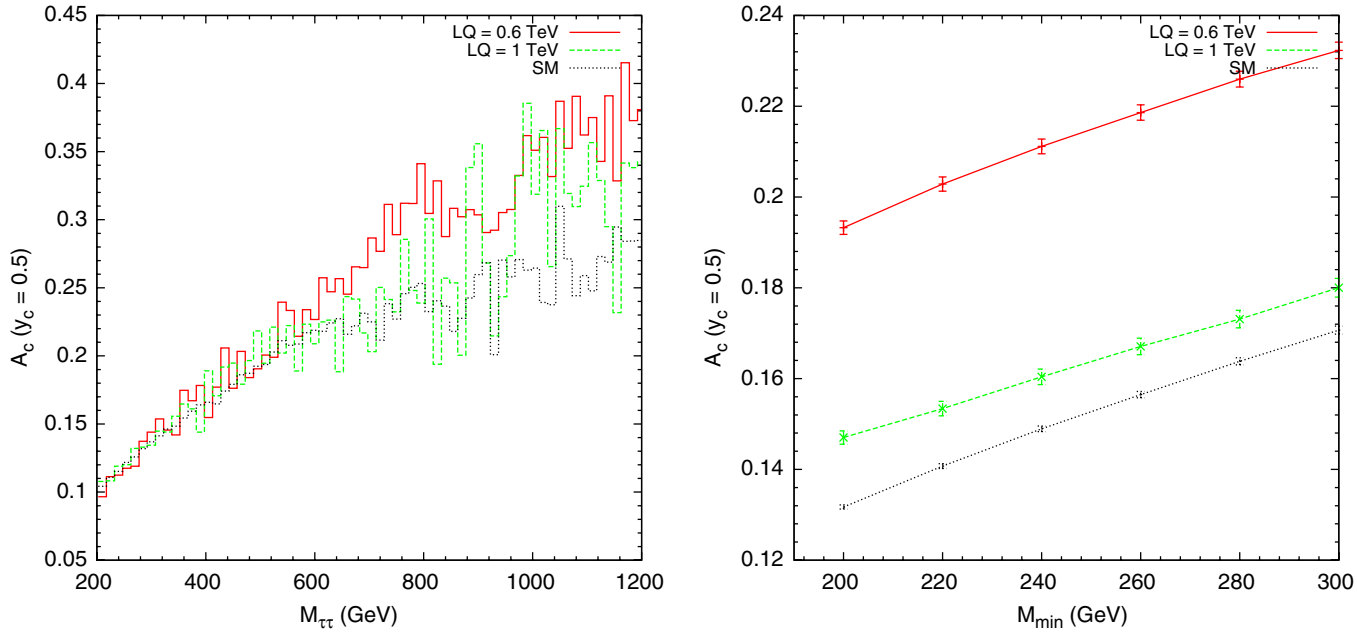

FIG. 9 (color online). Integrated charge asymmetry for the lepto-quark model 1 (LQ-1) for $M_{LQ} = 0.6$, 1 TeV vs $M_{\tau\tau}$ (left) and integrated over $M_{\tau\tau} \geq M_{min}$ (right).

The most recent number obtained using this process corresponds to a lower bound on the lepto-quark mass near 50 TeV [26]. Although one must keep these indirect constraints in mind, they are not foolproof substitutes for direct searches; instead they yield complementary information.

In both scenarios we will show numerical results for lepto-quark masses of 600 GeV and 1 TeV which are within the direct reach of LHC but significantly below the indirect limits.

The additional contributions to the dilepton cross section are due to t-and u-channel exchange of lepto-quarks as illustrated in the Feynman diagrams shown in Fig. 7. In Table III we compare the τ-pair cross section that results in these models with the SM.

In Fig. 8 we show the dilepton-invariant mass distributions that result in both cases LQ-1 and LQ-2 for $M_{LQ} = 0.6$, 1 TeV, respectively. As expected, these distributions do not show any "bumps" as the lepto-quarks are not exchanged

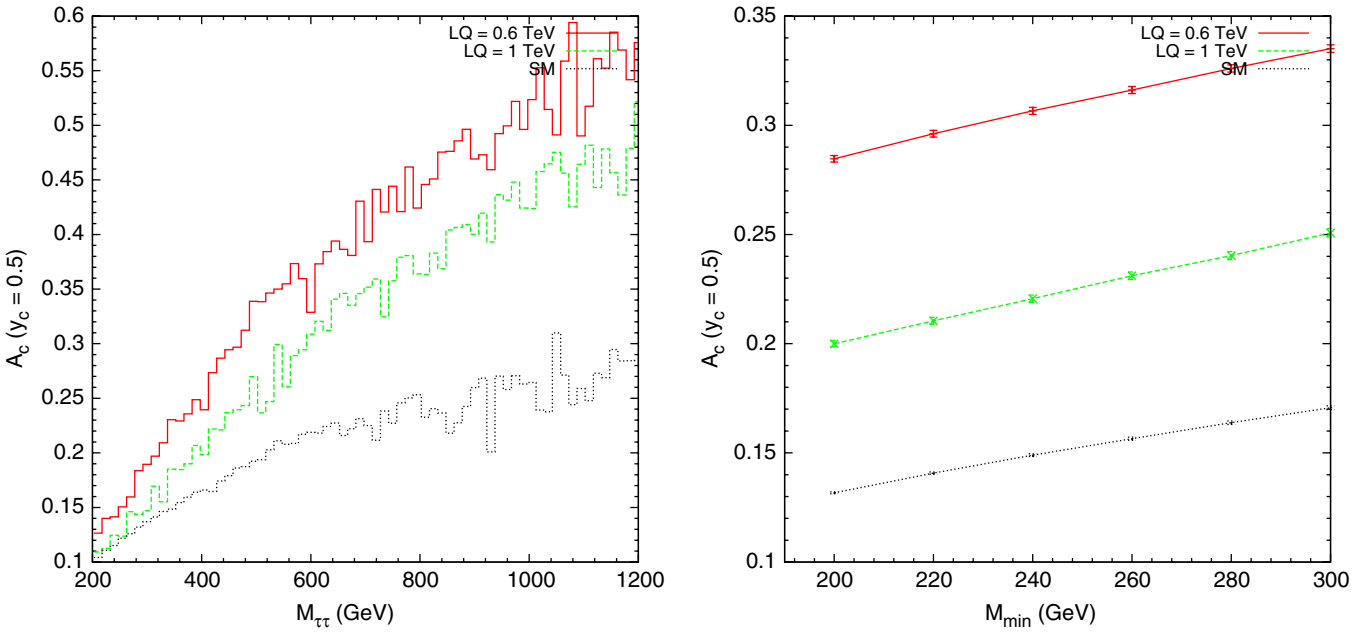

FIG. 10 (color online). Integrated charge asymmetry for the lepto-quark model 2 (LQ-2) for $M_{LQ} = 0.6$, 1 TeV vs $M_{\tau\tau}$ (left) and integrated over $M_{\tau\tau} \geq M_{min}$ (right).

TABLE IV. Integrated lepton charge asymmetry (in percent), $\mathcal{A}_c(y_c)$, for lepto-quark models 1, 2 (LQ-1, 2) and the SM with 1σ errors for 1 year of LHC data (at $\int \mathcal{L}dt = 10$ fb^{-1} per year). All numbers are for $y_c = 0.5$, and all masses are given in TeV.

Cuts	LQ-1		LQ-2		SM
	$M_{V_{2/3}} = 0.6$	$M_{V_{2/3}} = 1$	$M_{V_{5/3}} = 0.6$	$M_{V_{5/3}} = 1$	
$M_{\tau\tau} > 0.20$ TeV	19.3 ± 0.5	14.7 ± 0.6	28.5 ± 0.3	20.0 ± 0.5	13.2 ± 0.6
$M_{\tau\tau} > 0.22$ TeV	20.3 ± 0.5	15.3 ± 0.7	29.6 ± 0.3	21.0 ± 0.5	14.1 ± 0.7
$M_{\tau\tau} > 0.24$ TeV	21.1 ± 0.5	16.0 ± 0.7	30.7 ± 0.3	22.1 ± 0.5	14.9 ± 0.8
$M_{\tau\tau} > 0.26$ TeV	21.9 ± 0.6	16.7 ± 0.8	31.6 ± 0.4	23.1 ± 0.6	15.6 ± 0.9
$M_{\tau\tau} > 0.28$ TeV	22.6 ± 0.6	17.3 ± 0.8	32.6 ± 0.4	24.0 ± 0.6	16.4 ± 1.0
$M_{\tau\tau} > 0.30$ TeV	23.2 ± 0.6	18.0 ± 0.9	33.5 ± 0.4	25.1 ± 0.6	17.1 ± 1.1

in the s-channel. However, they do show an enhancement over the SM, particularly for the larger values of $M_{\tau\tau}$.

The results for the charge asymmetry are shown in Fig. 9 for scenario LQ-1 and in Fig. 10 for scenario LQ-2. In both cases we show the charge asymmetry integrated over rapidity for $|y| < y_c = 0.5$ as a function of dilepton-invariant mass as well as the asymmetry integrated over both rapidity and dilepton-invariant mass.

In Table IV we show the integrated τ-lepton charge asymmetry in percent for two different values of the lepto-quark mass in the two models discussed above as well as for the SM. We show results for $y_c = 0.5$ and for different values of $M_{\min}$ with their corresponding 1σ statistical error for an integrated luminosity of 10 fb^{-1} at $\sqrt{S} = 14$ TeV.

IV. ANALYSIS AT THE τ-LEPTON DECAY LEVEL

In the previous section we have identified a couple of models that produce τ-lepton charge asymmetries that can differ from the SM by factors of roughly two. In this section we study how the asymmetries are affected when the τ-lepton decay is taken into consideration. For this purpose it will suffice to compare the SM asymmetry with the one induced by the LQ-2 model with $M_{V_{5/3}} = 0.6$ TeV (the case resulting in the largest asymmetry in the analysis of the previous section).

We will consider the following τ-lepton decay modes:

(i) Same type dilepton mode. In this case both τ-leptons in the pair undergo leptonic decay into muons or electrons: $pp \to \tau^+\tau^- \to \ell^+\ell^- \not{E}_T$, $\ell = \mu, e$. The final state is thus a muon or electron pair plus missing transverse energy, $\not{E}_T$, due to invisible neutrinos. Since the τ-leptons are highly boosted, their decay products travel in essentially the same direction as the parent τ-lepton in the lab frame. The asymmetry is therefore constructed using the direction of the muons (or electrons) instead of the τ-leptons.
The background for this mode has two origins: the $\ell^+\ell^-$ pair can arise from $t\bar{t}$, W^+W^- or ZZ production, as was already the case with the analysis at the τ-lepton level; or it can arise from direct Drell-Yan production of $\ell^+\ell^-$. The only handle we have on this direct background is a requirement of missing energy. The available statistics in these two modes are decreased with respect to the number of τ pair events by about 94%: $B(\tau \to \ell\nu\bar{\nu})^2 \approx 0.03$.

(ii) Different type dilepton mode, or events with one muon and one electron: $pp \to \tau^+\tau^- \to \ell^+\ell'^- \not{E}_T$, $\ell, \ell' = \mu, e$, $\ell \neq \ell'$. These modes are the cleanest from the background perspective, suffering only from the same background already present in the τ-lepton level analysis: $t\bar{t}$, W^+W^-, or ZZ production. The available statistics in these modes is therefore about 6% of the available τ-lepton pairs.

(iii) Modes in which one τ-lepton decays leptonically to a muon or an electron and the other one hadronically. In the hadronic decays of highly boosted τ-leptons the resulting jet (j_τ) is also approximately collinear with the original τ-lepton. The asymmetry is thus constructed using the direction of the charged lepton (muon or electron) and the j_τ; with the sign of the corresponding τ-lepton charges being tagged by the lepton charge. The background for these modes consists of the same $t\bar{t}$, W^+W^-, or ZZ production present in the previous modes and in addition of W plus one jet (Wj) production. We will limit our analysis to the two hadronic decay modes $\tau^\pm \to \pi^\pm\nu$ and $\tau^\pm \to \rho^\pm\nu$ which together account for a branching ratio near 36%. The available statistics in these modes is therefore around 25% of the available τ-lepton pairs.
For the Wj background that meets our selection cuts, we assume a probability of 0.3% that the QCD jet will fake a τ jet and reduce these events accordingly. This number is taken from studies by ATLAS and CMS [27].

In all cases we generate the signal and background events using HADGRAPH [11] and implement the τ-lepton decay modes with the package DECAY [28]. We use the following basic cuts on the leptons and the jets: $p_T > 6$ GeV, $|\eta| < 2.5$ and $\Delta R_{ik} < 0.4$, where the indices $i, k = \ell, j$.

A. Results for dilepton modes

In Fig. 11 we show the charge asymmetry in the dilepton (same type) channel for both the LQ-2 model with two

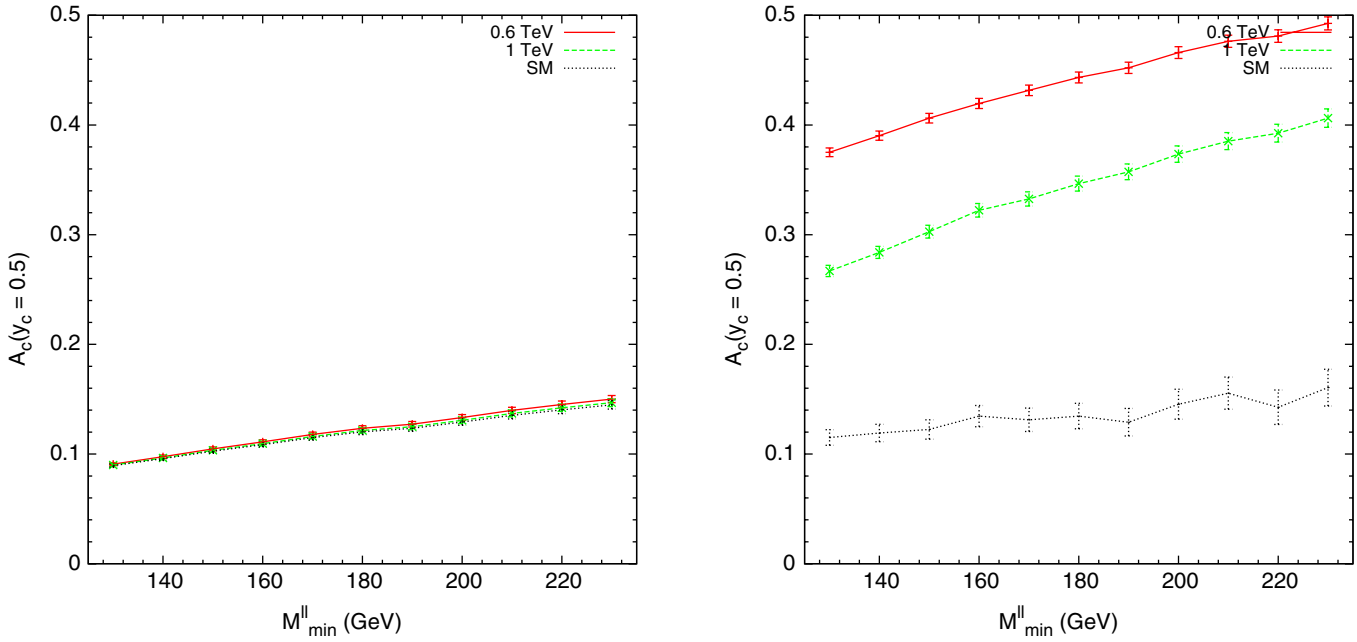

FIG. 11 (color online). Charge asymmetry in the dilepton mode *with same lepton flavor pair* for the SM and the LQ-2 model with two different lepto-quark masses as a function of a minimal $M_{\ell\ell}$ cut without (left) and with (right) an additional requirement of missing E_T as described in the text.

values of lepto-quark mass and for the SM. The curve on the left shows that the direct Drell-Yan background overwhelms the signal in this case, whereas the curve on the right shows the improvement achieved by requiring missing energy, $E_T > 10$ GeV in the event. We show our results for the dimuon mode, but at our level of analysis the results for e^+e^- are identical. The asymmetry is shown for $y_c = 0.5$ as discussed in the previous section. The asymmetry is integrated over the invariant mass of the dimuon pair with a minimal value that replaces the mimimal value of $M_{\tau\tau}$ in the previous section. We show a range for $M_{\ell\ell}$ from 130 GeV to 230 GeV. The lower end of this range is

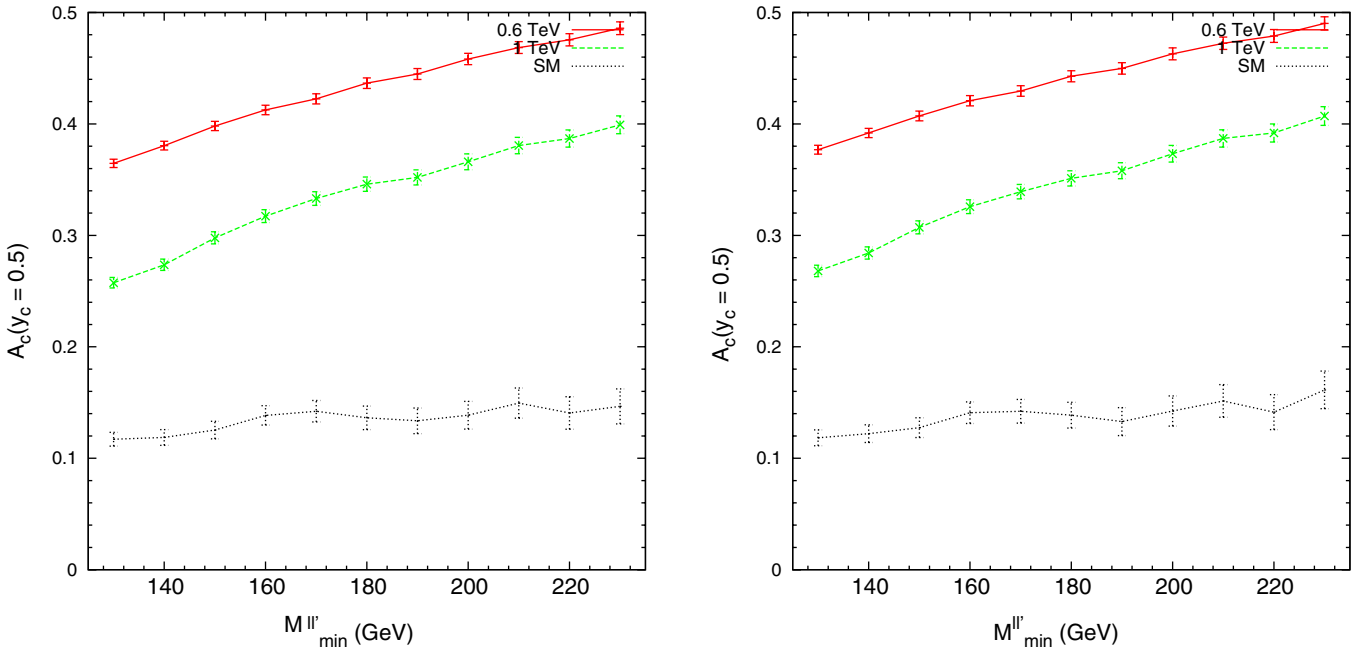

FIG. 12 (color online). Charge asymmetry in the dilepton mode *with different lepton flavor pair* for the SM and the LQ-2 model with two different lepto-quark masses as a function of a minimal $M_{\ell\ell}$ cut without (left) and with (right) an additional requirement of missing E_T as described in the text.

TABLE V. Integrated lepton charge asymmetry $\mathcal{A}_{\ell\ell'}$ (in percent) for the LQ-2 model and the SM with $M_{\rm min}^{\ell\ell'} = 130$ GeV (a) without (left table) and (b) with the requirement of a minimum missing E_T (right table). The 1σ errors correspond to statistics for one year of LHC data (at $\int \mathcal{L}dt = 10$ fb^{-1} per year). All the masses are given in TeV.

(ℓ, ℓ')	LQ-2 Model		SM
	$M_{V_{5/3}} = 0.6$	$M_{V5/3} = 1$	
(μ^+, μ^-)	9.1 ± 0.5	9.0 ± 0.6	8.9 ± 0.6
(e^+, e^-)	9.2 ± 0.5	9.1 ± 0.6	9.1 ± 0.6
(e^+, μ^-)	36.2 ± 1.6	25.6 ± 2.0	12.1 ± 2.3
(μ^+, e^-)	36.5 ± 1.6	25.8 ± 2.0	11.7 ± 2.3

(ℓ, ℓ')	LQ-2 Model		SM
	$M_{V_{5/3}} = 0.6$	$M_{V5/3} = 1$	
(μ^+, μ^-)	37.5 ± 1.7	26.7 ± 2.2	11.5 ± 2.4
(e^+, e^-)	37.7 ± 1.7	26.6 ± 2.2	12.4 ± 2.4
(e^+, μ^-)	37.4 ± 1.7	26.6 ± 2.2	12.2 ± 2.4
(μ^+, e^-)	37.7 ± 1.7	26.8 ± 2.2	11.8 ± 2.4

chosen to remove the Z resonance where the SM cross section peaks and the upper end is simply chosen for illustration.

In Fig. 12 we show the charge asymmetry in the dilepton (different type) channel for both the LQ-2 model with two values of lepto-quark mass and for the SM. In this case we show the results for μ^+e^- and note that, at our level of analysis, the results for μ^-e^+ are identical. In this case there is no direct Drell-Yan background, so the requirement of missing E_T does not improve our signal to background ratio. The asymmetry is once again shown for $y_c = 0.5$, integrated over the invariant mass of the dilepton pair.

The integrated charge asymmetries for the four dilepton channels are given in Table V without the missing E_T requirement in left table and with the additional $\not{E}_T > 10$ GeV requirement in the right table. This missing energy requirement only affects the e^+e^- and $\mu^+\mu^-$ modes where it removes the direct Drell-Yan background. The errors shown in the tables are the statistical errors corresponding 10 fb^{-1}. These results show the usefulness of the

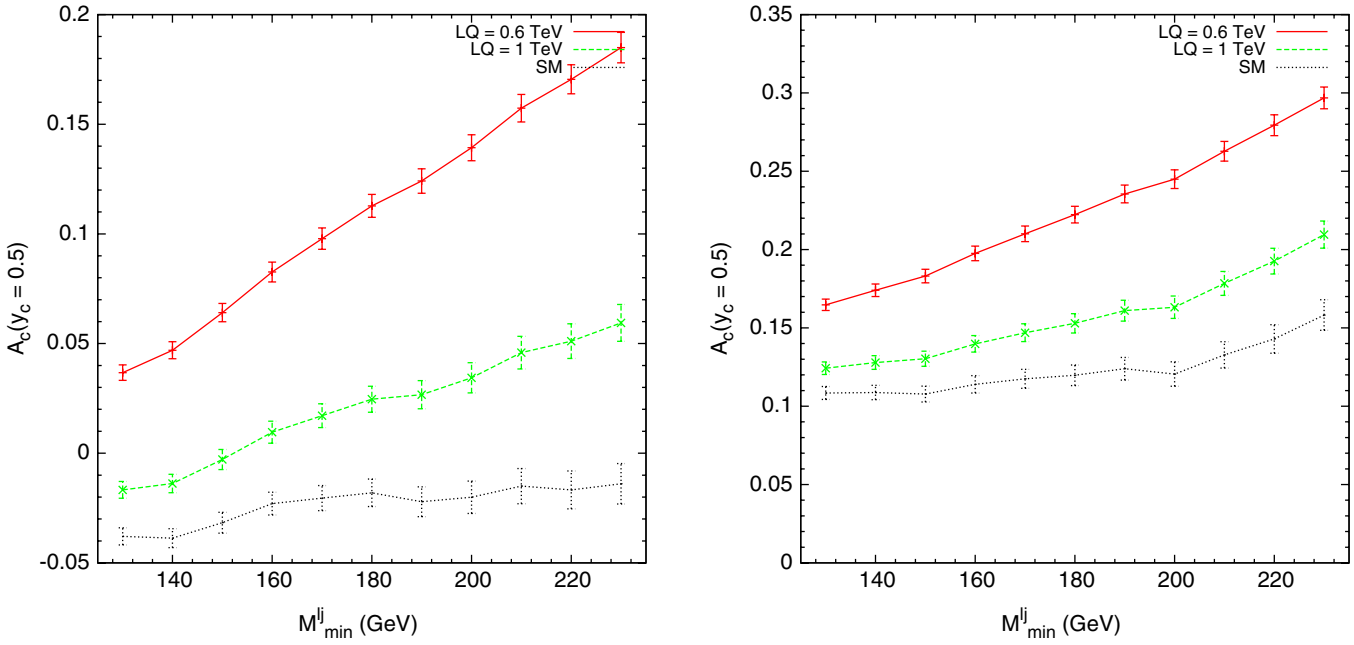

FIG. 13 (color online). Charge asymmetry in the dilepton mode *with same lepton flavor pair* for the SM and the LQ-2 model with two different lepto-quark masses as a function of a minimal $M_{\ell\ell}$ cut without (left) and with (right) an additional requirement of missing E_T as described in the text.

TABLE VI. Integrated lepton charge asymmetry $\mathcal{A}_{\ell j}$ (in percent) for the LQ-2 model and the SM with $M_{\min}^{\ell j} = 130$ GeV with the missing E_T requirement. The 1σ errors correspond to statistics for one year of LHC data (at $\int \mathcal{L} dt = 10$ fb^{-1} per year). All the masses here are given in TeV.

	LQ-2 Model		SM
	$M_{V_{5/3}} = 0.6$	$M_{V5/3} = 1$	
(ℓ^+, j)	3.7 ± 0.4	-1.7 ± 0.4	-3.7 ± 0.4
(j, ℓ^-)	16.5 ± 0.4	12.4 ± 0.4	10.9 ± 0.4

charge asymmetry as a discriminator for new physics affecting the τ-lepton.

B. Results for the ℓj_τ modes

These modes suffer from the additional Wj background in which the QCD jet fakes a τ jet. This background is very significant even after we reduce it by assuming a 0.3% misidentification rate and this is evident in the difference between the results for $\ell^+ j$ and $\ell^- j$ in Figs. 13 between left and right figures. We can understand the difference between these asymmetries qualitatively because the Wj background events themselves have an asymmetry that is different for $W^+ j$ and $W^- j$, -6.3% and 11%, respectively, with our cuts. In addition, the background is larger for $\ell^+ j$ since $\sigma(W^+ j) > \sigma(W^- j)$ at pp colliders.

The results for the integrated asymmetries in these two cases are presented in Table VI requiring the events to have $\not{E}_T > 10$ GeV. The missing E_T requirement is not very important in this case.

These results show that the ℓj_τ channel is less promising for using the charge asymmetry as a discriminator of new physics, but that it can still serve to distinguish some models.

Interestingly, the asymmetries in the $\ell^\pm j$ channels, with the $W^\pm j$ background removed at the Monte Carlo level, are not the same as those in the $\ell^+ \ell'^-$ channels. This is due to the different effect of requiring the same minimum invariant mass for $\ell\ell'$ and ℓj, with the cut in $\ell\ell'$ being more efficient at rejecting SM background. The difference is simply due to the different kinematics for two-body decay vs three-body decay. As a consequence of this difference it would be difficult to combine the different channels to improve the statistical error even if the $W^\pm j$ background could be controlled effectively.

V. SUMMARY AND CONCLUSION

The forward-backward asymmetry has been a very useful tool to obtain information about the SM couplings of fermions to the Z boson. At the LHC it will not always be possible to reconstruct a forward-backward asymmetry, but some of the same information can be obtained from charge asymmetries. In this paper we have emphasized that the charge asymmetry can also play an important role in the search for new physics in τ-pair production at the LHC.

We have investigated some kinematic properties of this charge asymmetry concluding that a value of y_c near 0.5 is optimal in this case. The asymmetry can be constructed as a function of lepton-pair-invariant mass, $M_{\tau\tau}$, but a better probe of new physics is obtained by integrating the charge asymmetry over the available $M_{\tau\tau}$ range with a minimum cut, $M_{\min}$. Originally this cut serves the purpose of removing the SM Z background. We found that the integrated asymmetry increases by increasing $M_{\min}$ far above the M_Z, although at the cost of lost statistics. We have explored the optimal value of $M_{\min}$ in the context of two examples.

We have illustrated two generic scenarios of new physics models that single out the τ-lepton and would not show up in $\mu^+\mu^-$ or e^+e^- pair production. We discuss a nonuniversal Z' as an example of a new resonance that prefers to decay into tau leptons. We also considered certain leptoquarks as an example of nonresonant new physics. They single out the tau lepton by associating the third-generation leptons with the first-generation quarks. We have illustrated examples of new physics that can induce τ charge asymmetries that are easy to distinguish from the SM.

We have first presented an analysis of the charge asymmetry at the $\tau^+\tau^-$ level based on the premise that $\tau^+\tau^-$ samples have already been identified by the experiments. To back up our conclusions we have also studied selected τ decays with their associated backgrounds. We find that the dilepton modes are very clean to study the charge asymmetry. The lepton plus jet modes are less sensitive, but can still provide some discriminating power in the charge asymmetry.

In conclusion we find that an experimental study of the τ-lepton charge asymmetry at the LHC can provide valuable information in the search for new physics. Clearly a detector level study by the experimental collaborations will be necessary to accurately quantify the possibilities of this proposal, and we encourage both ATLAS and CMS to conduct such studies.

ACKNOWLEDGMENTS

This work was supported in part by DOE under Contract No. DE-FG02-01ER41155. We thank David Atwood for useful discussions.

[1] Many papers have been devoted to the interpretation of this result. A couple that emphasize its significance are M. S. Chanowitz, Phys. Rev. Lett. **87**, 231802 (2001); W. J. Marciano, AIP Conf. Proc. **870**, 236 (2006).

[2] T. Han, G. Valencia, and Y. Wang, Phys. Rev. D **70**, 034002 (2004).

[3] G. Valencia and S. Willenbrock, Phys. Rev. D **50**, 6843 (1994).

[4] ALEPH Collaboration, DELPHI Collaboration, and L3 Collaboration, Phys. Rep. **427**, 257 (2006).

[5] V. M. Abazov *et al.* (D0 Collaboration), Phys. Rev. Lett. **100**, 142002 (2008); T. Aaltonen *et al.* (CDF Collaboration), Phys. Rev. Lett. **101**, 202001 (2008).

[6] J. H. Kuhn and G. Rodrigo, Phys. Rev. D **59**, 054017 (1999); M. T. Bowen, S. D. Ellis, and D. Rainwater, Phys. Rev. D **73**, 014008 (2006); O. Antunano, J. H. Kuhn, and G. Rodrigo, Phys. Rev. D **77**, 014003 (2008); S. Jung, H. Murayama, A. Pierce, and J. D. Wells, Phys. Rev. D **81**, 015004 (2010); R. Diener, S. Godfrey, and T. A. W. Martin, Phys. Rev. D **80**, 075014 (2009); V. Barger, W. Y. Keung, and C. T. Yu, Phys. Rev. D **81**, 113009 (2010).

[7] M. Aharrouche (ATLAS Collaboration), Acta Phys. Pol. Supp. **1**, 257 (2008).

[8] CMS physics analysis summary in http://cdsweb.cern.ch/record/1279615.

[9] P. Ferrario and G. Rodrigo, J. Phys. Conf. Ser. **171**, 012091 (2009).

[10] S. Catani, G. Ferrera, and M. Grazzini, J. High Energy Phys. 05 (2010) 006.

[11] T. Stelzer and W. F. Long, Comput. Phys. Commun. **81**, 357 (1994); J. Alwall *et al.*, J. High Energy Phys. 09 (2007) 028.

[12] T. Sjostrand, S. Mrenna, and P. Z. Skands, J. High Energy Phys. 05 (2006) 026.

[13] J. Pumplin, D. R. Stump, J. Huston, H. L. Lai, P. M. Nadolsky, and W. K. Tung, J. High Energy Phys. 07 (2002) 012.

[14] M. Pioppi (CMS Collaboration), Nucl. Phys. B, Proc. Suppl. **189**, 311 (2009).

[15] B. Gosdzik (ATLAS Collaboration), arXiv:1009.6135.

[16] For a recent review see P. Langacker, Rev. Mod. Phys. **81**, 1199 (2009).

[17] X. G. M. He and G. Valencia, Phys. Rev. D **70**, 053003 (2004); **74**, 013011 (2006); C. W. Chiang, N. G. Deshpande, and J. Jiang, J. High Energy Phys. 08 (2006) 075; R. Mohanta and A. K. Giri, Phys. Rev. D **79**, 057902 (2009); V. Barger, L. Everett, J. Jiang, P. Langacker, T. Liu, and C. Wagner, Phys. Rev. D **80**, 055008 (2009); V. Barger, L. L. Everett, J. Jiang, P. Langacker, T. Liu, and C. E. M. Wagner, J. High Energy Phys. 12 (2009) 048; N. G. Deshpande, X. G. He, and G. Valencia, Phys. Rev. D **82**, 056013 (2010).

[18] E. Ma, Phys. Lett. B **433**, 74 (1998); E. Ma and D. P. Roy, Phys. Rev. D **58**, 095005 (1998).

[19] X. G. He and G. Valencia, Phys. Rev. D **66**, 013004 (2002); **66**, 079901(E) (2002); **68**, 033011 (2003).

[20] A. Arhrib, K. Cheung, C. W. Chiang, and T. C. Yuan, Phys. Rev. D **73**, 075015 (2006); S. K. Gupta and G. Valencia, Phys. Rev. D **82**, 035017 (2010); R. Diener, S. Godfrey, and T. A. W. Martin, Phys. Rev. D **83**, 115008 (2011).

[21] S. Davidson, D. C. Bailey, and B. A. Campbell, Z. Phys. C **61**, 613 (1994); M. Hirsch, H. V. Klapdor-Kleingrothaus, and S. G. Kovalenko, Phys. Lett. B **378**, 17 (1996).

[22] M. Leurer, Phys. Rev. D **49**, 333 (1994).

[23] J. C. Pati and A. Salam, Phys. Rev. D **10**, 275 (1974); **11**, 703(E) (1975).

[24] K. Nakamura *et al.* (Particle Data Group), J. Phys. G **37**, 075021 (2010).

[25] M. Leurer, Phys. Rev. D **50**, 536 (1994); R. Foot and G. Filewood, Phys. Rev. D **60**, 115002 (1999); M. Kuze and Y. Sirois, Prog. Part. Nucl. Phys. **50**, 1 (2003); **53**, 679 (2004).

[26] F. Abe *et al.* (CDF Collaboration), Phys. Rev. Lett. **81**, 5742 (1998); T. Aaltonen *et al.* (CDF Collaboration), Phys. Rev. Lett. **102**, 201801 (2009).

[27] G. Bagliesi, arXiv:0707.0928.

[28] J. Alwall, P. Artoisenet, S. de Visscher, C. Duhr, R. Frederix, M. Herquet, and O. Mattelaer, AIP Conf. Proc. **1078**, 84 (2009).